

Induction of Bleb Structures in Lipid Nanoparticle Formulations of mRNA Leads to Improved Transfection Potency

Miffy Hok Yan Cheng,* Jerry Leung, Yao Zhang, Colton Strong, Genc Basha, Arash Momeni, Yihang Chen, Eric Jan, Amir Abdolazadeh, Xinying Wang, Jayesh A. Kulkarni, Dominik Witzigmann, and Pieter R. Cullis*

The transfection potency of lipid nanoparticle (LNP) mRNA systems is critically dependent on the ionizable cationic lipid component. LNP mRNA systems composed of optimized ionizable lipids often display distinctive mRNA-rich “bleb” structures. Here, it is shown that such structures can also be induced for LNPs containing nominally less active ionizable lipids by formulating them in the presence of high concentrations of pH 4 buffers such as sodium citrate, leading to improved transfection potencies both in vitro and in vivo. Induction of bleb structure and improved potency is dependent on the type of pH 4 buffer employed, with LNP mRNA systems prepared using 300 mM sodium citrate buffer displaying maximum transfection. The improved transfection potencies of LNP mRNA systems displaying bleb structure can be attributed, at least in part, to enhanced integrity of the encapsulated mRNA. It is concluded that enhanced transfection can be achieved by optimizing formulation parameters to improve mRNA stability and that optimization of ionizable lipids to achieve enhanced potency may well lead to improvements in mRNA integrity through formation of the bleb structure rather than enhanced intracellular delivery.

silencing pathological genes and mRNA for expressing therapeutic proteins.^[1] Major examples include Onpattro,^[2] an LNP formulation of siRNA to treat transthyretin-induced amyloidosis approved by the Food and Drug Administration in 2018, and the COVID-19 mRNA vaccines that have received regulatory approval in many jurisdictions worldwide.^[3] There are many more LNP RNA therapeutics in development^[4] with potential applications ranging from treating atherosclerosis^[5] to cancer^[6] to heart failure.^[7]

LNP formulations of siRNA and mRNA for in vivo applications are composed of ionizable cationic lipids, phospholipids, cholesterol, and polyethylene glycol (PEG)-lipids.^[8] The ionizable lipid component plays a critical role in determining transfection potency and considerable effort has gone into synthesizing progressively optimized ionizable lipids. For example, the gene silencing potency of LNP siRNA to silence FVII in hepatocytes

(following an i.v. injection) ranges from an ED₅₀ of ≈ 40 mg kg⁻¹ (supporting information to Semple et al.^[9]) for 1,2-dioleoyl-3-dimethylammonium-propane (DODAP), the first ionizable cationic lipid employed^[10] to ≈ 1 mg kg⁻¹ for 1,2-dilinoleoyloxy-

1. Introduction

Lipid nanoparticle (LNP) systems are enabling nucleic-acid-based therapeutics such as short interfering RNA (siRNA) for

M. H. Y. Cheng, J. Leung, C. Strong, G. Basha, A. Momeni, Y. Chen, E. Jan, P. R. Cullis
Department of Biochemistry and Molecular Biology
University of British Columbia
Vancouver, British Columbia V6T 1Z4, Canada
E-mail: miffy.cheng@ubc.ca; pieterc@mail.ubc.ca

J. Leung, C. Strong
Michael Smith Laboratories
University of British Columbia
Vancouver, British Columbia V6T 1Z4, Canada

Y. Zhang
School of Biomedical Engineering
University of British Columbia
Vancouver, British Columbia V6T 1Z4, Canada

A. Abdolazadeh, X. Wang, J. A. Kulkarni, D. Witzigmann, P. R. Cullis
NanoVation Therapeutics Inc.
2405 Wesbrook Mall, Vancouver, British Columbia V6T 1Z3, Canada

The ORCID identification number(s) for the author(s) of this article can be found under <https://doi.org/10.1002/adma.202303370>

© 2023 The Authors. Advanced Materials published by Wiley-VCH GmbH. This is an open access article under the terms of the Creative Commons Attribution-NonCommercial-NoDerivs License, which permits use and distribution in any medium, provided the original work is properly cited, the use is non-commercial and no modifications or adaptations are made.

DOI: 10.1002/adma.202303370

N,N-dimethyl-3-aminopropane (DLinDMA)^[11] to 0.01 mg kg⁻¹ for DLinKC2DMA (KC2)^[9] and finally to 0.005 mg kg⁻¹ for DLinMC3DMA (MC3).^[12] MC3 is the ionizable lipid employed in Onpatro. In the case of LNPs for delivery of mRNA, these synthetic efforts have continued, using gene expression in the liver as the measure of transfection potency. This has resulted in second-generation lipids such as ALC-0315 and SM-102. LNP systems incorporating ALC-0315 and SM-102, which are the ionizable lipids employed in the Pfizer/BioNTech and Moderna COVID-19 mRNA vaccines, respectively, exhibit up to tenfold higher gene expression in the liver than can be achieved with LNPs containing MC3.^[13]

In contrast to the efforts made to develop optimized ionizable cationic lipids, few studies have attempted to optimize the formulation process. In this regard, the first step in the formulation of LNP–nucleic acid systems involves rapid mixing of the lipids in ethanol with a pH 4 buffer containing the nucleic acid to be encapsulated. The pH 4 buffer is required to protonate the ionizable lipid, thus inducing a positive charge. Following the mixing step, the solution is dialyzed against phosphate-buffered saline (PBS) to remove ethanol and raise the pH to 7.4.^[14] During the dialysis process, three variables are changed at once—removal of ethanol, an increase in pH, and an increase in ionic strength. The increase in pH results in the conversion of the ionizable lipid from the positively charged form to the neutral form, which engenders fusion between the small vesicles formed at pH 4.^[15] This fusion process is regulated by the PEG–lipid content, when the PEG–lipid content in the outer monolayer reaches a critical value, further fusion is inhibited, thus limiting the size.^[16]

In this work, we show that the small vesicles formed at pH 4 will fuse in the presence of high concentrations of pH 4 buffers, indicating that the fusion process to reach the limiting size can also be triggered by the presence of high ionic strengths at pH 4. We then show that larger LNP mRNA systems consistent with fusion events can be induced during the mixing process by mixing the lipids in ethanol into high-concentration pH 4 buffers containing the mRNA. Interestingly, when the pH is then adjusted to pH 7.4 by dialysis against PBS, the resulting LNP mRNA systems are significantly more transfection potent both *in vitro* and *in vivo*. They also exhibit enhanced formation of bleb structures as detected by cryo-transmission electron microscopy (cryo-TEM) as compared to LNP mRNA systems prepared in lower concentration pH 4 buffers. The improvements for LNP mRNA systems containing nominally less potent ionizable lipids can be particularly notable. For example, by optimizing the concentration and type of pH 4 buffer, LNP mRNA systems encoding firefly luciferase (LNP luc mRNA) containing KC2 can exhibit *in vivo* transfection potencies that are comparable or superior to those achieved for LNPs containing SM-102. This gain in transfection competence is attributed to enhanced mRNA stability when sequestered into bleb structures in the LNPs.

2. Results

2.1. High Concentrations of pH 4 Buffers Induce Bleb Structures in LNP mRNA Systems

In order to choose the types and concentrations of pH 4 buffer to generate fusion during the ethanol/water mixing stage, we

first investigated the fusion properties of the small “limit size” vesicles formed when an ethanol solution of KC2/1,2-distearoyl-*sn*-glycero-3-phosphocholine (DSPC)/cholesterol/(*R*)-2,3-bis(tetradecyloxy)propyl-1-(methoxy polyethylene glycol 2000) carbamate (PEG-DMG) (50/10/38.5/1.5 mol%) was dispersed into a 25 mM NaOAc pH 4 buffer.^[15] LNPs containing trace amounts of either DiI or DiO were generated separately, then mixed together and dialyzed into various concentrations of NaOAc, Na-citrate phosphate (CitPhos), and Na-citrate buffers. Fusion was monitored by fluorescent resonance energy transfer (FRET).^[17] Upon excitation at 485 nm (excitation wavelength of DiO), a FRET signal can be observed at 590 nm (emission wavelength for DiI) if the labels are in close proximity. As noted in Figure S1 in the Supporting Information, the citrate buffer is the most fusogenic buffer, requiring a concentration of only ≈20 mM to produce complete fusion. Acetate buffers were the least fusogenic, requiring a concentration of ≈300 mM to achieve complete fusion.

LNP mRNA systems with the lipid composition KC2/DSPC/cholesterol/PEG-DMG (50/10/38.5/1.5 mol%) were then formulated with pH 4 buffers containing luciferase mRNA (N/P = 6) in either 25 mM NaOAc or 300 mM NaOAc, CitPhos, or Na-citrate and subsequently dialyzed against PBS, pH 7.4. Encapsulation efficiencies greater than 90% were achieved. High concentrations of pH 4 buffer gave rise to size increases from ≈45 to ≈60 nm diameter (Figure 1a and Table S1, Supporting Information).

The KC2 LNP luc mRNA systems prepared in the different pH 4 buffers were incubated with Huh7 cells and the luminescence was assayed at 24 h. As shown in Figure 1b, incubation with LNPs prepared in 300 mM pH 4 NaOAc buffer resulted in a 32-fold increase in luminescence (LNP mRNA concentration 0.3 μg mRNA mL⁻¹) as compared to using LNPs prepared in 25 mM NaOAc. Further, an additional twofold improvement was observed if the pH 4 buffer employed was 300 mM Na-citrate. This increase in transfection potency cannot be attributed to increased uptake as shown in Figure S2 in the Supporting Information.

In an effort to understand causes of the improved transfection potencies of LNP mRNA systems prepared in high-concentration pH 4 buffers, we characterized their structural properties using cryo-TEM. LNP luc mRNA systems prepared in the presence of 25 mM NaOAc displayed the “solid core” morphology (Figure 1d, white arrows) described previously.^[15] However, increasing the NaOAc ionic strength to 300 mM resulted in a fraction of particles that exhibited bleb structures with a distinctive mottled texture. The prevalence of these structures was sensitive to the type of pH 4 buffer employed (Figure 1e–g, yellow arrows). KC2 LNP luc mRNA systems prepared in 300 mM NaOAc, 300 mM CitPhos, or 300 mM Na-citrate displayed 5%, 44%, and 59% bleb structure, respectively (Figure 1c). Titration of the pH 4 citrate buffer revealed that formulating with concentrations as low as 5 mM led to significant induction of bleb structure and enhancement in transfection potency (see Figure S3a–c, Supporting Information).

Previous work suggests that the blebs with the mottled appearance correspond to polar regions in the LNPs that contain mRNA.^[18] It is logical to propose that the smallest bleb structures contain only one copy of mRNA. Inspection of the cryo-TEM images of Figure 1f,g obtained for the LNP luc mRNA prepared in

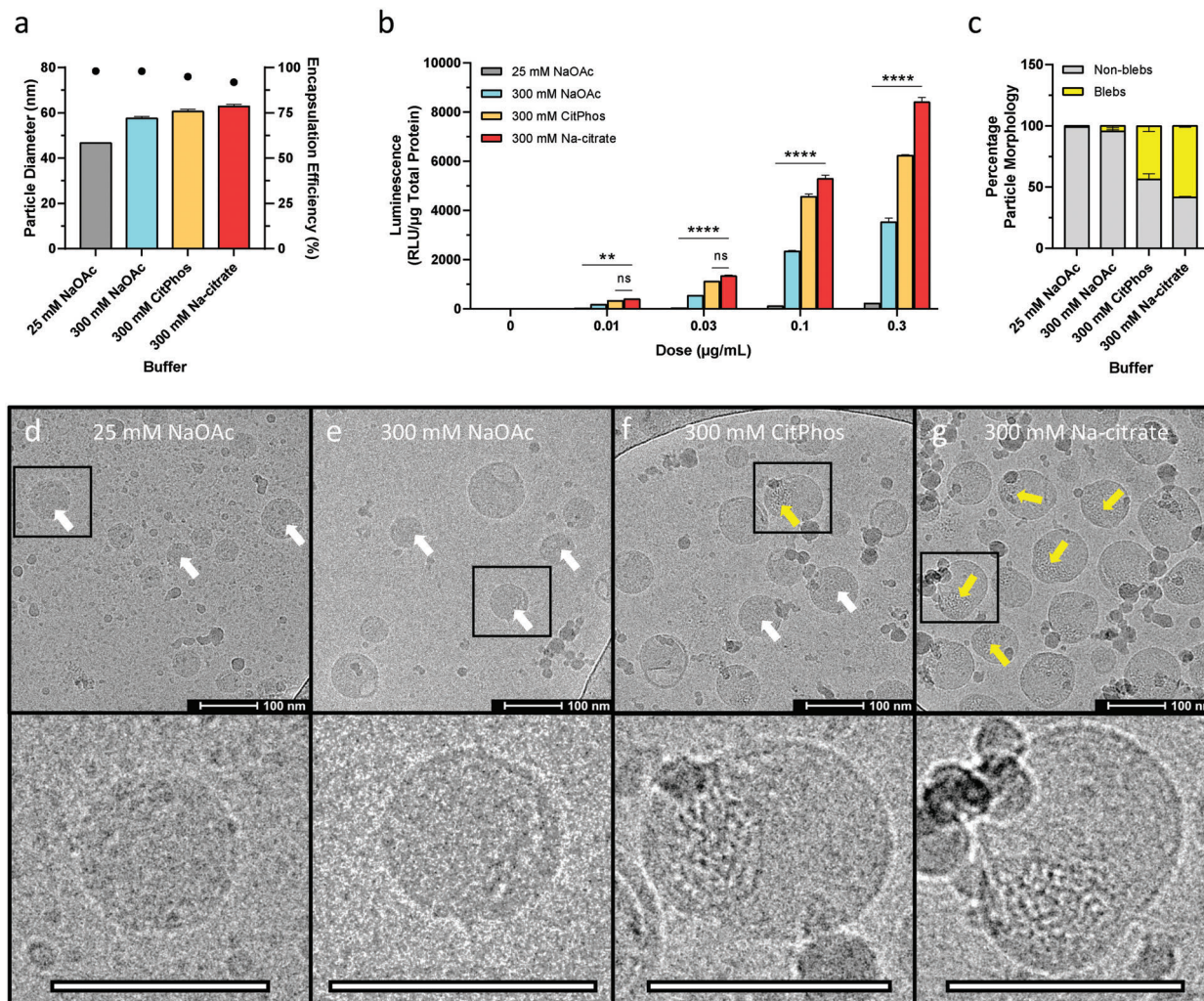


Figure 1. Formulation of KC2 LNP luc mRNA systems in high concentrations of pH 4 buffers leads to the formation of bleb structures and improved in vitro transfection potencies. LNP luc mRNA systems (N/P = 6) with the lipid composition KC2/DSPC/cholesterol/PEG-DMG (50/10/38.5/1.5 mol%) were prepared using various pH 4 buffers as described in the Experimental Section. a) Size and encapsulation efficiency of LNP luc mRNA systems formulated with various pH 4 buffers. Data were analyzed through a two-way ANOVA, **** p < 0.0001. b) Luminescence of Huh7 cells incubated for 24 h with LNP luc mRNA systems formulated with various pH 4 buffers (mean \pm standard error of the mean (S.E.M.), n = 3). Data were analyzed through a two-way ANOVA, ^{ns} non-significance, ** p < 0.01, and **** p < 0.0001. c) Percentage of bleb and nonbleb structural morphology of LNP luc mRNA formulated with various pH 4 buffers (mean \pm SD, n = 3). Data were analyzed through a two-way ANOVA, **** p < 0.0001. d–g) Cryo-TEM images of LNP luc mRNA formulated with various pH 4 buffers: d) 25 mM NaOAc, e) 300 mM NaOAc, f) 300 mM CitPhos, and g) 300 mM Na-citrate. The white arrows point to LNPs exhibiting normal solid core structure whereas the yellow arrows indicate bleb structures. White scale bar for enlarged images = 100 nm.

the presence of 300 mM CitPhos or Na-citrate indicates a minimum cross-sectional area associated with the blebs of 233 nm². This value is consistent with the theoretical cross-sectional area of \approx 200 nm² for a 2 kb mRNA in condensed, spherical form, assuming an mRNA diameter of 2 nm and a length per nucleotide of 0.33 nm.^[19] Assuming that essentially all of the encapsulated mRNAs exists in bleb structures for LNP mRNA systems prepared in the presence of 300 mM Na-citrate (Figure 1g) and that the area per monomer is 233 nm², it may be calculated that the average number of copies of mRNA encapsulated per LNP is 5.7 (Table S2, Supporting Information). This may be compared to the theoretical value of an average of 4.5 copies of luc mRNA per LNP for the \approx 60% (see Figure 1c) of LNPs that do contain mRNA

as evidenced by the presence of blebs. This estimate assumes an encapsulation efficiency of 80%, an N/P value of 6, a lipid density of 0.9 g mL⁻¹, and an LNP diameter of 60 nm. For details see the mRNA copies per LNP spreadsheet in the Supporting Information.

2.2. The Presence of Bleb Structures also Depends on the Species of Ionizable Lipid

To characterize the influence of the type of ionizable lipid on bleb structure, we examined the influence of high ionic strength pH 4 buffers on the structure and in vitro transfection potency

of LNP luc mRNA systems containing MC3 as well as the second-generation lipids ALC-0315 and SM-102. LNP luc mRNA formulations containing MC3, ALC-0315, and SM-102 were prepared using 25 mM NaOAc and 300 mM Na-citrate and then incubated with Huh7 cells. Increases in luminescence of 20-, four-, and twofold over that achieved for the 25 mM NaOAc buffer were observed for LNP luc mRNA systems prepared in the 300 mM Na-citrate buffer and containing MC3, ALC-0315, or SM-102, respectively (Figure 2a). As noted in Figure 1a, formulation of KC2 LNP luc mRNA systems in 300 mM Na-citrate resulted in a 64-fold improvement in transfection potency in vitro over that achieved using a 25 mM NaOAc buffer (LNP luc mRNA concentration 0.3 $\mu\text{g mRNA mL}^{-1}$). Thus, the improvements in transfection potency, while substantial, were not as dramatic as achieved for the KC2-containing LNP systems, particularly for LNPs containing the second-generation lipids ALC-0315 or SM-102. Of particular interest, the KC2 LNP luc mRNA system prepared in 300 mM Na-citrate was nearly twofold more potent than the LNP systems containing ALC-0315 and SM-102 prepared in the presence of 300 mM Na-citrate. Some formulation differences were noted as the MC3 and ALC-0315-containing LNPs increased in size significantly and displayed poorer encapsulation efficiencies when formulated using 300 mM Na-citrate whereas LNP luc mRNA containing SM-102 did not increase in size and exhibited excellent encapsulation properties (Figure 2b and Table S3, Supporting Information).

Cryo-TEM studies again supported the correlation between the presence of blebs and enhanced transfection potency. MC3 LNP mRNA formulated in 25 mM NaOAc resulted in a small amount of bleb structure (2%), whereas a large increase in bleb structure (76%) was observed when formulated in 300 mM Na-citrate. Similarly, LNPs containing SM-102 exhibited low levels (4%) of bleb structures when formulated using the 25 mM NaOAc buffer and higher levels (21%) when prepared using 300 mM Na-citrate. However, for LNPs containing ALC-0315, appreciable bleb structure (53%) was observed even for the LNP prepared using the 25 mM NaOAc pH 4 buffer (Figure 2c–i). Much larger structures with large blebs were observed when LNPs containing ALC-0315 were formulated using the 300 mM Na-citrate buffer. Theoretical calculations using the spreadsheet in the Supporting Information indicate that LNP mRNA systems exhibiting a diameter of 45 nm formulated at an N/P of 6 should contain 1.4 luc mRNA per particle whereas larger systems of 75 or 125 nm diameter should contain on average ≈ 6.5 and ≈ 30 mRNA per LNP assuming 100% encapsulation efficiency and that all the LNPs contain mRNA.

2.3. LNP mRNA Systems Exhibiting Bleb Structures Exhibit Improved In Vivo Transfection Properties

We next determined whether the improved in vitro transfection properties for LNPs prepared using 300 mM pH 4 Na-citrate were also observed in vivo. LNP luc mRNA systems containing KC2 and SM-102 were formulated in either 25 mM NaOAc pH 4 or 300 mM Na-citrate pH 4 and administered intravenously (i.v.) into CD-1 mice at an mRNA dose of 0.5 mg kg^{-1} . Bioluminescence was assayed at 3, 6, and 24 h post-injection. As shown in Figure 3, both systems

formulated using the 300 mM Na-citrate pH 4 buffer exhibited significantly improved gene expression in the liver and spleen compared to LNPs prepared using the 25 mM NaOAc buffer.

Gene expression was particularly improved for the KC2 LNP luc mRNA system. At 3 h post-injection, the abdominal bioluminescence observed for the KC2 LNP luc mRNA system prepared using the 300 mM Na-citrate buffer was enhanced more than 40-fold compared to the signal achieved for the same system prepared using 25 mM NaOAc (Figure 3a,b). While the SM-102 LNP luc mRNA systems prepared using the 300 mM Na-citrate buffer also gave rise to higher luminescence than the same system prepared using 25 mM NaOAc, the increase was only fivefold. As a result, the KC2 LNP luc mRNA system prepared using the Na-citrate buffer exhibited superior transfection properties when compared to the LNPs containing SM-102.

Transfection levels for the KC2 LNP luc mRNA system prepared using the 300 mM pH 4 buffer were also improved at 6 h post-injection (Figure 3c,d). The abdominal bioluminescence for mice receiving KC2 LNP luc mRNA prepared using 300 mM pH 4 Na-citrate was more than 300-fold higher than in mice receiving KC2 LNP luc mRNA prepared using 25 mM NaOAc. Again, the KC2 LNP luc mRNA 300 mM Na-citrate system produced slightly higher luminescence than the corresponding SM-102 LNP luc mRNA system. Finally, significant bioluminescence remained at 24 h for both the KC2 LNP luc mRNA and the SM-102 LNP luc mRNA systems prepared in 300 mM Na-citrate (Figure 3e,f).

At 24 h post-injection, the mice were sacrificed and dissected, and transfection was assayed using ex vivo IVIS (in vivo imaging system) imaging for heart, lungs, liver, kidney, adrenal, brain, skin, fat, muscle, and bone tissue. As shown in Figure S4a in the Supporting Information, significant luminescence was detected in each organ and tissue. The signal from the spleen is particularly notable for the LNP luc mRNA systems prepared using the 300 mM Na-citrate pH 4 buffer. The spleen luminescence observed following administration of KC2 LNP luc mRNA is more than 200-fold greater than for the same system prepared using the 25 mM NaOAc buffer (Figure S4b, Supporting Information). The SM-102 LNP luc mRNA system prepared in the 300 mM Na-citrate buffer also exhibited a strong spleen signal but only a ninefold increase compared to the same system prepared using the 25 mM NaOAc buffer (Figure S4c, Supporting Information). The fluorescence from the DiD-labeled LNPs also revealed higher spleen uptake of the 300 mM Na-citrate system over the 25 mM NaOAc system, possibly due to the larger size of the LNPs prepared using high citrate concentrations (Figure S4d, Supporting Information).

Finally, experiments were conducted to establish that the enhanced potency of the LNP mRNA systems prepared in 300 mM citrate pH 4 buffers did not result in enhanced toxicity as compared to systems prepared using the 25 mM NaOAc buffer. CD-1 mice were injected i.v. with LNP luc mRNA at an mRNA dose of 1.5 mg kg^{-1} , three times higher than used for the gene expression studies of Figure 3. No significant difference in hematology, biochemistry, or cytokine profile was observed 24 h post-injection between the two LNP formulations. Organs such as heart, lung, liver, spleen, and kidney were excised for

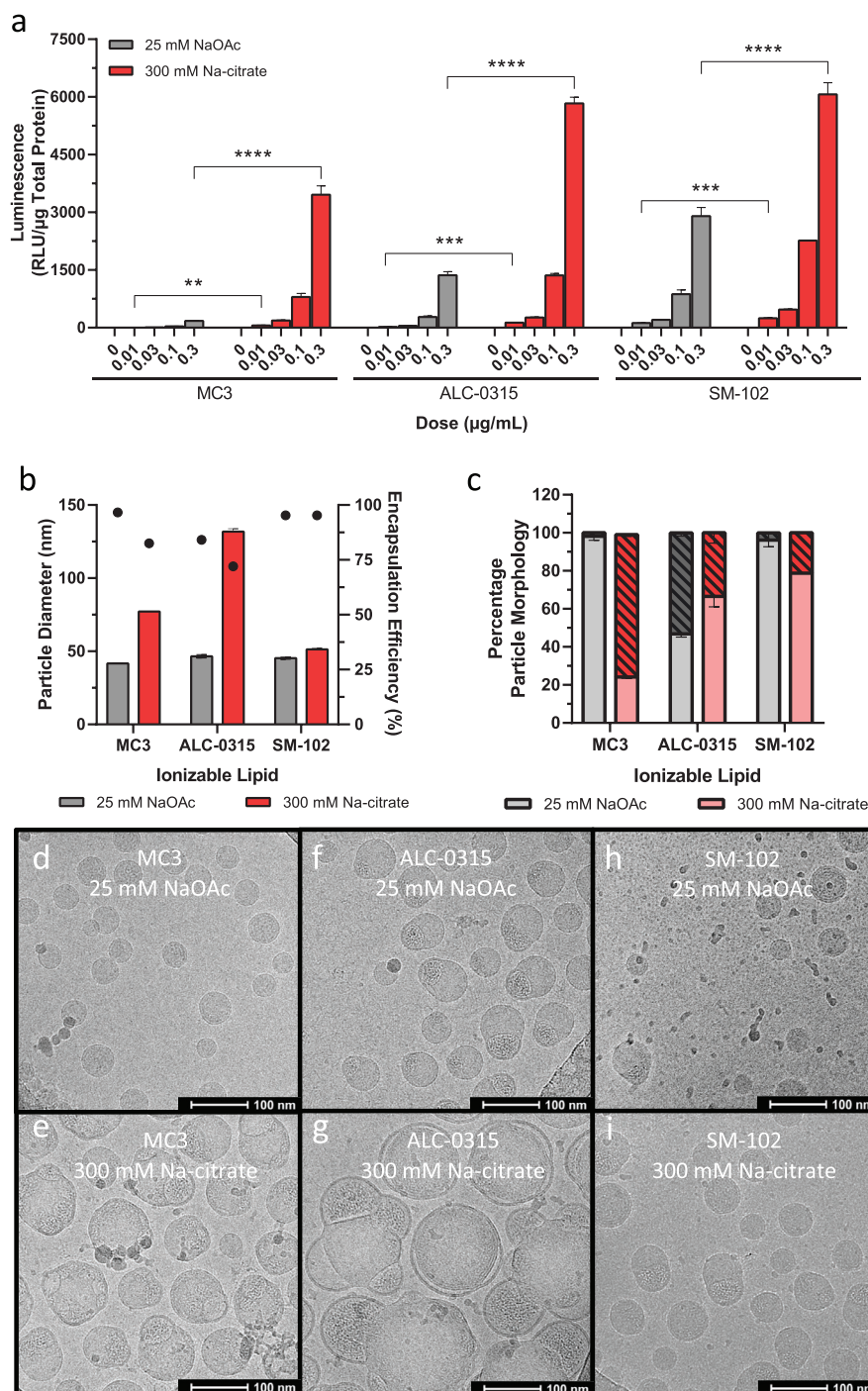


Figure 2. The improvement in LNP luc mRNA transfection potency in vitro when formulated in high concentrations of pH 4 buffer depends on the species of ionizable lipid employed. LNP luc mRNA systems (N/P = 6) with the lipid composition ionizable lipid/DSPC/cholesterol/PEG-DMG (50/10/38.5/1.5 mol%) were prepared containing various ionizable lipids as described in the Experimental Section. a) Luminescence of Huh7 cells incubated for 24 h with LNP luc mRNA systems ($0.01\text{--}0.3\ \mu\text{g mRNA mL}^{-1}$) containing different ionizable cationic lipids and formulated with 25 mM NaOAc or 300 mM Na-citrate pH 4 buffers (mean \pm S.E.M., $n = 3$). Data were analyzed by two-tailed unpaired *t*-test for doses of 0.01 and 0.3 $\mu\text{g mRNA mL}^{-1}$. $**p < 0.01$, $***p < 0.001$, $****p < 0.0001$. b) Influence of ionizable lipid content and pH 4 buffer on LNP luc mRNA size (bars, left y-axis) and encapsulation efficiency (dots, right y-axis). c) Percentage of bleb (striped) and nonbleb (nonstriped) structural morphologies of LNP luc mRNA systems formulated with different ionizable lipids. d–i) Cryo-TEM images of MC3 LNP luc mRNA formulated in d) 25 mM NaOAc and e) 300 mM Na-citrate; f, g) ALC-0315 LNP luc mRNA formulated in 25 mM NaOAc (f) and 300 mM Na-citrate (g); and h, i) SM-102 LNP luc mRNA formulated in 25 mM NaOAc (h) and 300 mM Na-citrate (i).

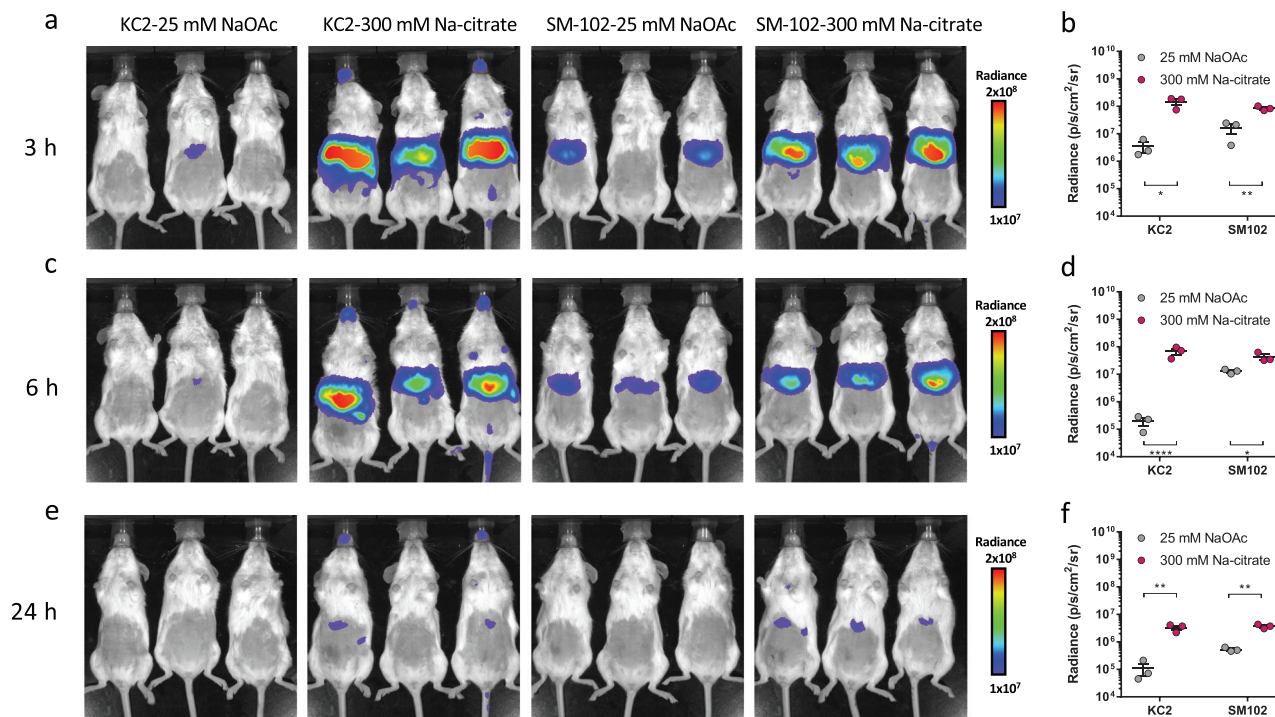


Figure 3. LNP luc mRNA systems prepared using 300 mM Na-citrate pH 4 buffer induce improved gene expression in vivo compared to LNP luc mRNA systems prepared using 25 mM NaOAc. KC2 LNP luc mRNA and SM-102 LNP luc mRNA systems were formulated using either 300 mM Na-citrate pH 4 buffer or 25 mM NaOAc pH 4 buffer and administered i.v. at an mRNA dose of 0.5 mg kg^{-1} to CD-1 mice. a,c,e) Bioluminescence was assayed using IVIS imaging at 3 h post-injection (a), 6 h post-injection (c), and 24 h post-injection (e). b,d,f) Quantified abdominal radiance at 3, 6, and 24 h post-injection (mean \pm S.E.M., $n = 3$). Data were analyzed through a two-tailed unpaired *t*-test. * $p < 0.05$, ** $p < 0.01$, and **** $p < 0.0001$.

hematoxylin and eosin (H&E) staining. No differences were observed between the control and treatment groups (Figure S5a–d, Supporting Information).

2.4. Higher Concentrations of pH 4 Buffer Lead to Fusion and Formation of Larger Structures

As noted, the presence of high concentrations of citrate ions during the dilution/rapid mixing step will cause fusion of positively charged vesicles formed at pH 4, similar to the way that Ca^{2+} causes fusion of negatively charged vesicles.^[20] This leads to a difference in morphology at pH 4 and pH 7.4 of KC2-containing LNP mRNA systems prepared using 25 mM NaOAc and 300 mM Na-citrate. As shown in Figure 4a–d, cryo-TEM studies revealed the presence of larger structures when LNPs were formulated directly under 300 mM Na-citrate at pH 4, with essentially the same size as the LNP mRNA systems achieved following dialysis against PBS to raise the pH to 7.4. These structures exhibit empty blebs surrounded on the exterior by a lipid bilayer. This fusion process to form larger structures with empty blebs at pH 4 can also be observed for the small vesicles formed in 25 mM NaOAc pH 4 buffers (in the presence of mRNA) by dialyzing against 300 mM NaOAc, CitPhos, and Na-citrate buffers (Figure S6, Supporting Information).

2.5. Induction of Bleb Structure Results in Enhanced Integrity of Encapsulated mRNA

In an effort to understand the reason why LNP mRNA systems containing bleb structures exhibit enhanced transfection potencies, the integrity of mRNA prepared in LNPs formulated in the 25 mM NaOAc pH 4 buffer was compared to mRNA in LNP mRNA prepared using the 300 mM NaOAc, CitPhos, and Na-citrate buffer that have been incubated in the presence of serum for up to 24 h. As shown in Figure S7 in the Supporting Information and summarized in Figure 4e, a BioAnalyzer analysis of the mRNA integrity indicated that the mRNA formulated in LNPs using the 300 mM Na-citrate pH 4 buffer is significantly less susceptible to breakdown than mRNA formulated in the 25 mM NaOAc pH 4 buffer.

In order to determine the influence of the enhanced mRNA stability on the translational capabilities of the mRNA, mRNA was extracted from the LNPs following incubation with serum and the translational activity was assayed in a cell-free wheat germ extract. The mRNA extracted from LNP mRNA systems formulated in the high-concentration pH 4 buffers was tenfold or more translationally competent than mRNA extracted from LNPs formulated in the 25 mM NaOAc buffer (Figure 4f). The improvement in activity for the systems formulated in buffers such as 300 mM Na-citrate likely arises due to improved integrity of the mRNA encapsulated in these systems.

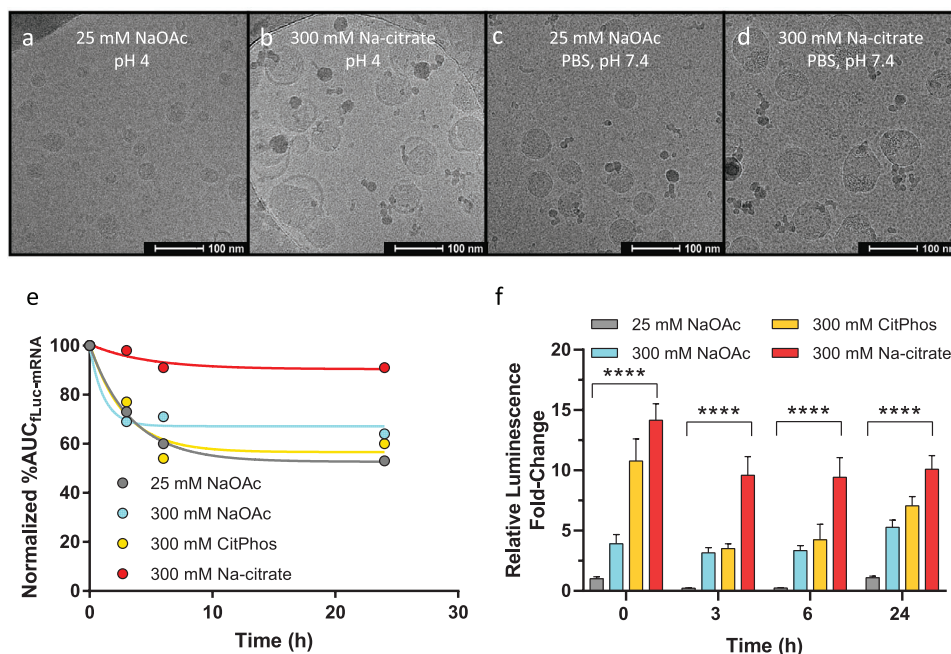


Figure 4. Formulation of LNP luc mRNA systems using 300 mM Na-citrate pH 4 buffer leads to fusion and formation of larger LNP systems at pH 4 as compared to LNP prepared in 25 mM NaOAc. a–d) LNP luc mRNA systems (N/P = 6) with the composition KC2/DSPC/cholesterol/PEG-DMG (50/10/38.5/1.5 mol%) were formulated in 25 mM NaOAc or 300 mM Na-citrate and imaged at pH 4 (a,b), and then were dialyzed against PBS and imaged at pH 7.4 (c,d). e) mRNA extracted from LNP luc mRNA systems formulated using the 25 mM NaOAc pH 4 buffer displays lower mRNA integrity when incubated in 50% FBS over time as compared to all other 300 mM buffer systems. f) Luc mRNA extracted from LNP luc mRNA systems prepared in high-concentration pH 4 buffers shows significantly higher translation competence in cell-free wheat germ lysate than mRNA extracted from LNP luc mRNA systems prepared using the 25 mM NaOAc pH 4 buffer, (mean \pm S.E.M., $n = 6$). Data were analyzed through a two-way ANOVA, **** $p < 0.0001$.

3. Discussion

The results presented here show that bleb structures can be induced in LNP mRNA systems by preparing in the presence of high concentrations of pH 4 buffer and that these systems exhibit enhanced transfection properties both in vitro and in vivo. There are three areas that warrant further discussion. The first topic concerns the mechanism whereby the presence of high-concentration pH 4 buffers induces bleb structures and why this results in enhanced transfection potency. The second area concerns the mechanism whereby some species of ionizable lipids induce bleb structures even at low concentrations of pH 4 buffer. Finally, we discuss the correlation between the bleb areas and theoretical estimates of mRNA content, which offers a new way of estimating the number of copies of mRNA per LNP.

With regard to the mechanism of induction of bleb structures, the data presented support the model shown in Figure 5. This model builds on the observation that the presence of high ionic strength pH 4 buffers induces fusion of smaller vesicles initially formed on dilution of ethanol into aqueous media to achieve a size that is limited by the PEG–lipid content (Figure S6, Supporting Information). The presence of “empty” blebs in these systems suggests phase separation of the positively charged ionizable lipid and mRNA into the electron-dense core, leaving DSPC/cholesterol-rich bilayer structures to form the blebs. This is consistent with the cryo-TEM structure of the core in empty LNPs prepared in 300 mM Na-citrate shown in Figure S8 in the

Supporting Information. The LNPs prepared containing MC3, KC2, and SM-102 in the presence of 300 mM Na-citrate clearly show internalized lipid in an organized phase that could reflect the presence of lamellar or cubic phase lipid^[21] among other possibilities. The migration of the mRNA cargo into the polar bleb would be predicted as the ionizable lipids progressively adopt the neutral form, dissociate from the mRNA and phase separate into a “solid core” oil droplet.

The reason why segregation of mRNA into bleb structures maintains the translation competence of the mRNA remains to be elucidated. Previous work has shown that formulated mRNA can form nucleotide-ionizable lipid adducts^[22] or can be damaged via oxidation or alkylation,^[23] sequestration into bleb structures may shield the mRNA from such events. It is also possible that factors influencing mRNA structure could play a role. Finally, the high concentrations of Na-citrate may play an important role in segregating the ionizable lipid, and also may act as a reducing agent to suppress downstream mRNA degradation by quenching Mg²⁺-induced RNA fragmentation.^[24]

The observation of bleb structures for LNP mRNA systems prepared in 25 mM NaOAc and containing second-generation lipids such as ALC-0315 (Figure 2f) suggests that optimization efforts aimed at developing ionizable lipids for improved transfection may well be optimizing their ability to promote bleb structure and thus enhanced mRNA stability rather than improved intracellular delivery. Ionizable lipids such as ALC-0315 and SM-102 exhibit pronounced “cone” shapes due to their branched acyl chain composition and would be expected to favor adoption of

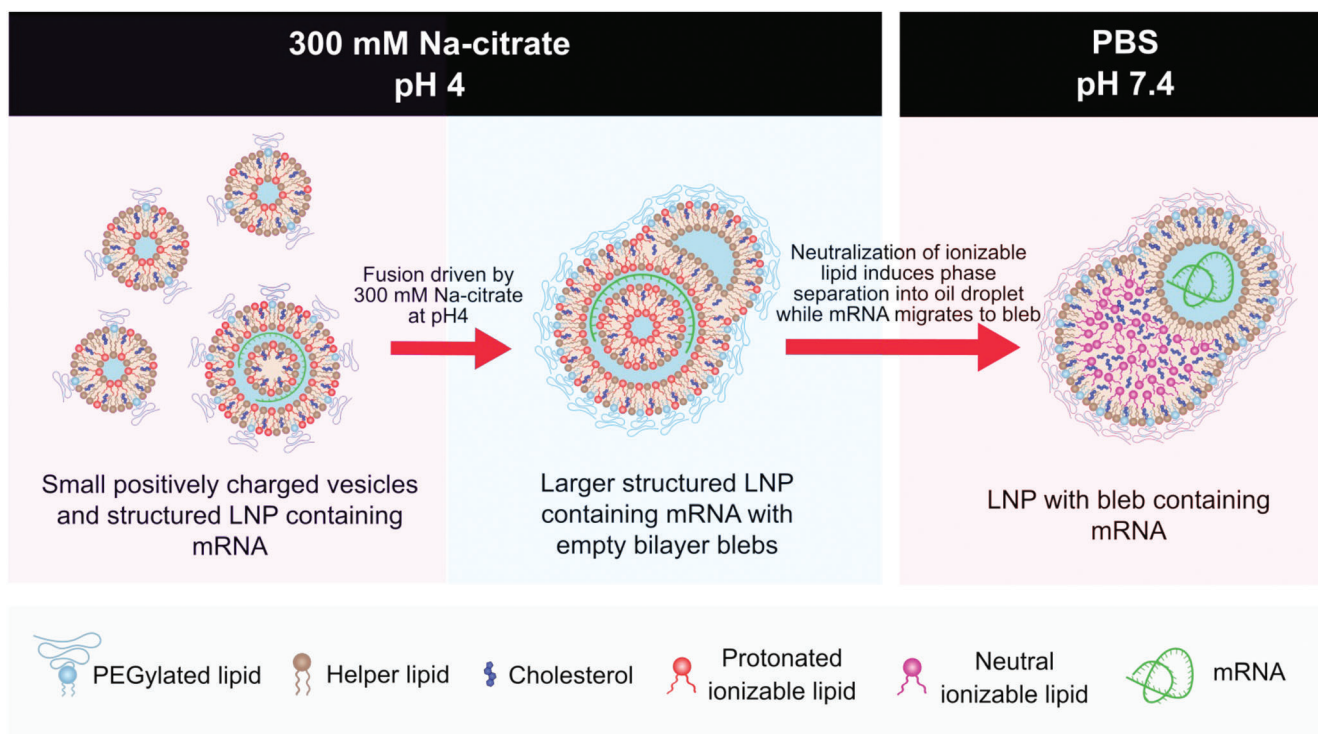


Figure 5. Mechanism of formation of the LNP mRNA systems exhibiting bleb structures. It is proposed that the presence of high concentrations of pH 4 buffers such as citrate causes fusion of the small vesicles and LNPs containing the mRNA initially produced on dilution of lipids in ethanol into an aqueous media. This fusion process results in larger structures where the size is limited by the increasing concentration of PEG–lipid on the surface as the ratio of surface lipid to core lipid decreases. The formation of blebs as observed in Figure 4b is ascribed to citrate and mRNA-induced segregation of the positively charged ionizable lipid into the core of the LNPs, leaving DSPC and associated cholesterol to form the monolayer around the LNPs and the exterior bilayer of the bleb. Subsequently raising the pH to 7.4 on dialysis against PBS results in phase separation of the neutral form of the ionizable lipid into a hydrophobic oil droplet core and migration of the mRNA into the polar interior of the bleb region.

phases such as the cubic or hexagonal H_{II} structures.^[25] Further, vesicles containing such lipids would be expected to fuse readily to form larger LNPs at pH 4. This is consistent with the fact that empty LNPs containing ALC-0315 and SM-102 form larger lipid structures when formulated using the 25 mM NaOAc pH 4 buffer than LNPs containing KC2 and MC3 (Figure S8, Supporting Information).

It is interesting that induction of bleb structures in systems containing “first generation” lipids such as KC2 can result in LNP mRNA systems that are more transfection potent than LNP mRNA systems containing ALC-0315 or SM-102. This finding suggests that screening of libraries of nominally less potent ionizable lipids to evaluate bleb formation and transfection potency following formulation in high-concentration pH 4 buffers could reveal highly transfection potent lipids. In any event, formulation in high concentrations of citrate buffer would be expected to enhance the transfection properties of LNP systems containing ionizable lipids generally.

The last discussion point concerns the fact that the areas of the blebs in the LNP mRNA systems correlates well with the areas predicted theoretically assuming one, two, or more copies of mRNA per LNP. These findings indicate, e.g., that more than 60% of LNP mRNA systems contain one or more copies of mRNA in the KC2 LNP mRNA formulation (N/P = 6) prepared in 300 mM Na-citrate pH 4. It would appear that induction of

bleb structures provides a method for determining the mRNA content per LNP that has not been available previously. Further refinement of the formulation protocols could allow the generation of LNP mRNA systems containing well-defined numbers of copies of mRNA with minimized presence of “empty” LNPs.

4. Conclusions

We have shown that LNP mRNA systems formulated using high-concentration pH 4 buffers exhibit bleb structure and enhanced transfection potencies. For LNPs containing nominally less active ionizable lipids, formulating them in the presence of high concentrations of Na-citrate pH 4 buffer leads to dramatically improved transfection potencies both in vitro and in vivo. The sequestration of mRNA into bleb structures is shown to maintain mRNA translation competency which likely accounts for the improvement in transfection potency. Finally, quantitation of bleb structures offers a new way to estimate mRNA content in LNP mRNA formulations.

5. Experimental Section

The lipids DSPC and PEG-DMG were purchased from Avanti Polar Lipids. The ionizable lipids DLinkC2DMA and DLinkMC3DMA were

purchased through Dr. Marco Ciufolini, while the ionizable lipids ALC-0315 and SM-102 were purchased from Cayman Chemicals. Cholesterol was purchased from Sigma Aldrich. Dulbecco's modified Eagle medium (DMEM) and fetal bovine serum (FBS) were purchased from Thermo Fisher Scientific. All other chemicals were purchased from Sigma Aldrich unless otherwise stated. Firefly Luciferase mRNA (ARCA Capped, 5mCTP, ψ UTP) was purchased from ApexBio or provided by NanoVation Therapeutics Inc.

LNP Formulation and Characterization: LNP mRNA systems were formulated as previously described,^[17] with slight modifications. All formulations were formulated by first dissolving lipids (ionizable lipid, DSPC, cholesterol PEG-DMG) into ethanol to a final concentration of 10 mM and at a ratio of 50/10/38.5/1.5 mol%, respectively. The lipid mixture was then rapidly mixed with an aqueous solution of mRNA (amine-to-phosphate ratio (N/P) of 6) and various buffers (25 mM sodium acetate, 300 mM sodium acetate, 300 mM Na-citrate phosphate, or 300 mM Na-citrate) at pH 4 using a T-junction mixer at a 1:3 ethanol/water ratio and final flow rate of 20 mL min⁻¹. The resulting mixture was dialyzed overnight against >500-fold volume of pH 7.4 PBS unless stated otherwise, then sterile-filtered with a 0.2 μ m Supor membrane syringe filter (Pall Corporation, Mississauga, ON, Canada) and concentrated in 10K Amicon ultracentrifugation units (EMD Millipore Corporation, Billerica, MA, USA). Total lipid content was determined by extrapolation using the Cholesterol E Kit (Wako Diagnostics, Mountain View, CA, USA). Particle size was measured as the number mean average, determined via dynamic light scattering using the Malvern Zetasizer Nano ZS.

For FRET studies, LNPs were formulated as described but with the inclusion of 0.1 mol% of the lipophilic tracers DiO or Dil in the initial lipid mixture with no mRNA added to the aqueous buffer.

For in vitro studies, LNP mRNA systems were formulated as described above, but with the inclusion of 0.1 mol% of the lipophilic tracer Dil and mRNA encoding firefly luciferase. The encapsulation efficiency of the mRNA was quantified using the Quant-iT RiboGreen RNA Assay Kit (Wako Diagnostics, Mountain View, CA, USA).

For in vitro LNP uptake studies, 0.05 mol% of the lipophilic tracer DiO was included in the initial lipid mixture.

For in vivo bioluminescence imaging studies, 0.5 mol% of the lipophilic tracer DiD was included in the initial lipid mixture.

For empty LNP formulation, all procedure was followed as described above with the exception of no mRNA being added to the aqueous buffer.

FRET Measurements: LNPs were labeled with DiO or Dil. LNP–DiO/LNP–Dil mixtures (equimolar concentrations) were diluted between 0.0125, 0.025, 0.05, 0.125, 0.25, 0.5, 1.25, 2.5, 6.25, 12.5, 25, 50, 75, 100, 150, 300, 450 mM NaOAc, CitPhos, and Na-citrate buffer at pH 4. LNP samples were excited at the donor excitation wavelength (ex. 485 nm) and the emission was collected at 590 nm using a fluorescence plate reader. The resulting FRET spectrum from each set of experiments was normalized to the emission of the donor probe (LNP–DiO) under identical conditions. The FRET of the donor (DiO) to the acceptor (Dil) could be observed by the decrease in fluorescence at 528 nm and increase at 590 nm.

Cryo-TEM: The freshly prepared LNP luc mRNA was concentrated (20–25 mg mL⁻¹ of total lipid), added to glow-discharged copper grids (3–5 μ L), and plunge-frozen using an FEI Mark IV Vitrobot (FEI, Hillsboro, OR, USA) to generate vitreous ice. Grids were moved into a Gatan 70° cryo-tilt transfer system pre-equilibrated to at least –180 °C and then inserted into the microscope. An FEI LaB6 G2 TEM (FEI, Hillsboro, OR) operating at 200 kV under low-dose conditions was used to image all samples with an FEI Eagle 4 K CCD camera. All samples (unless otherwise stated) were imaged at 55 000 \times magnification with a nominal under-focus of 1–2 μ m to enhance contrast. All sample preparation and imaging were performed by the UBC Bioimaging Facility (Vancouver, BC). Cryo-TEM imaging for Figure S2 in the Supporting Information was carried out at 200 kV using FEI Tecnai G2 Twin TEM, equipped with FEI Eagle 4K bottom mount CCD camera and Gatan cryo sample holder. Samples were imaged at the low dose mode at 29 000 \times and 50 000 \times magnification levels.

Manual LNP Annotation of Cryo-TEM Images: Images acquired from cryo-TEM can be found in the Supporting Information (Cryo-TEM images). For each formulation of LNPs containing mRNA, >10 frames were selected

for annotation. Each of these images contained between 1 and 93 LNPs in the field of view. Each LNP was analyzed for its features related to the bleb structure and the total number of nanoparticles counted as either bleb or nonbleb. The annotations were marked using a color-coded number. An example can be found in the Supporting Information.

LNP sizes were measured on FIJI based on the longest diameter of each individual particle using a custom FIJI parameter created for the annotation process (4.685 pixel nm⁻¹). The diameters of the blebs (d_{bleb}) were measured based on the number of blebs and the distance from the edge of the bleb to the end of the mottled mass dense. The diameter of the LNPs (d_{LNP}) was defined as the sum of all diameters of blebs and the electron dense core. Each LNP was marked with a number to keep track between each frame and count. Average LNP sizes were obtained from the measurement of a minimum of 200 LNPs over all representative fields of view.

To calculate the number of copies of mRNA per LNP, it was assumed that a single mRNA in a bleb exists in a condensed, spherical form with a volume calculated assuming an mRNA diameter of 2 nm and a length per nucleotide of 0.33 nm.^[19] For a 2 kb mRNA, the radius (r) of the mRNA sphere could be calculated to be \approx 8 nm and the cross-sectional area (πr^2) \approx 200 nm². The number of copies of mRNA encapsulated per LNP was determined based on the average cross-sectional area of the blebs in the cryo-TEM images divided by the area per monomer.

Cell Culture and Treatments: A human hepatocarcinoma cell line (Huh7) was cultured and maintained in DMEM media supplemented with 10% FBS, at 37 °C under 5% CO₂. For transfecting with LNPs, 13 000 cells per well were seeded into 96-well microplates for 24 h before treating with the LNP luc mRNA at mRNA doses from 0 to 0.3 μ g mL⁻¹. Following 24 h of incubation, the media was removed, and cells were lysed with 100 μ L of Glo Lysis buffer (Promega, Madison, WI, USA). The lysates were mixed at a 1:1 ratio with luciferase substrate (Promega, Madison, WI, USA) and luminescence was quantified using a Spark Multimode Microplate reader (Tecan, Zürich, Switzerland). Luminescence readings were then normalized to the total protein content per well as determined using the Pierce BCA Protein Assay Kit (Thermo Fisher Scientific, Rockford, IL, USA), and transfection was calculated by normalizing to the luminescence values for untreated cells.

For measuring LNP uptake, Huh7 cells were seeded at 300 000 cells per well into 6-well microplates for 24 h before treating with LNP luc mRNA containing 0.05% DiO at an mRNA dose of 0.3 μ g mL⁻¹. Following 24 h of incubation, media was removed, and the cells were washed twice and re-suspended in 500 μ L FACS buffer (2% FBS, 0.1% sodium azide, and 1 mM ethylenediaminetetraacetic acid (EDTA)). LNP uptake was measured as the median fluorescence intensity using a BD CytoFLEX LX and CytExpert software. 20 000 events gated on the viable cell population were collected, and the data were analyzed using FlowJo.

Bioluminescence Imaging of LNP mRNA Luciferase Transfection: All animal protocols were approved by the Canadian Animal Care Committee and conducted in accordance with relevant UBC guidelines and regulations. Mice were maintained on a regular 12 h light/12 h dark cycle in a modified barrier animal facility at UBC. CD1 female mice aged between 6 and 8 weeks were used throughout.

Female CD-1 mice were individually weighed and imaged prior to intravenous (i.v.) injection of LNP luc mRNA (0.5 mg kg⁻¹ mRNA). At 3, 6, and 24 h post-injection, mice were administered D-luciferin substrate solution (150 mg kg⁻¹) intraperitoneally 10 min before bioluminescence imaging. Mice belonging to the same dosing groups ($n = 3$) were anesthetized with 3% isoflurane and placed on the imaging platform in a supine position while being maintained on 3% isoflurane via a nose cone. Mice were imaged 10 min post-administration of D-luciferin and imaged on the Xenogen IVIS Spectrum In Vivo Imaging System, with an exposure time of 10 s. Bioluminescence values were quantified by measuring the radiance (photons/s/cm²/steradian) in the whole animal, and for focal regions of interest (abdominal region) using the Living Image software program.

Immediately following the last imaging time point (24 h), mice were euthanized, and the liver, spleen, heart, kidney, lungs, adrenals, brain, skin, fat, muscle, and bone were collected and imaged ex vivo. Biolumines-

cence values were quantified by the radiance (photons/s/cm²/steradian) for each excised organ using the Living Image software program.

For biodistribution measured through fluorescence, each organ was dissected and homogenized under sterile conditions by passing through a 42 µm cell strainer using a syringe plunger into a Petri dish containing completed DMEM. Tissue homogenates were then incubated for 20 min at 37 °C. Cell suspensions obtained were washed twice with ice cold (4 °C) PBS followed by resuspension in 300 µL FACS buffer. LNP luc mRNA delivery was assessed based on the relative mean fluorescence intensity of DiD measured on histograms obtained from gated cell populations using a LSRII flow cytometer and the FACSDiva software, and analyzed by FlowJo following acquisition of 100 000 events after gating on viable cell populations.

Acute Toxicity Studies: To measure the toxicity of the formulations used in vivo, mice ($n = 3$) for four groups (KC2—25 mM NaOAc; KC2—300 mM Na-citrate; SM-102—25 mM NaOAc; SM-102—300 mM Na-citrate) were administered i.v. with 1.5 mg kg⁻¹ LNP luc mRNA formulated based on Onpatro composition and one group with saline as control. At 24 h post i.v. administration, 1 mL of blood was withdrawn through cardiac puncture. Blood was transferred to MiniCollect K2EDTA and VACUETTE Z Serum Clot Activator Tube with Gel Separator, respectively (Fisher Scientific, Ottawa, ON, Canada), and transferred to UBC Centre for Comparative Medicine for further processing. The blood samples for biochemistry panel were allowed to clot at room temperature for 30 min and centrifuged at 2000 rpm for 10 min. Serum was then transferred to Eppendorf tubes and kept at 4 °C. Custom hematology test, biochemistry tests, and Mouse Cytokine Multiplex Panel were performed by IDEXX BioAnalytics, Delta, BC, Canada and IDEXX BioAnalytics, MO, USA. Major organs (heart, lungs, liver, spleen, and kidney) were also excised at 24 h post-administration for histopathological analysis through H&E staining by Wax-it Histology Services Inc. (Vancouver, BC, Canada).

LNP luc mRNA Stability, mRNA Integrity, and Wheat Germ Extract Assay: KC2 LNPs containing luc mRNA were incubated in 50% FBS at 0, 3, 6, and 24 h at 37 °C at a final total lipid concentration of 10 µg mL⁻¹. Nonencapsulated mRNA incubated in either PBS or 50% FBS under the same conditions were used as controls. mRNA was extracted from the LNP luc mRNA formulations with 50% FBS using a PureLink RNA Mini Kit (Thermo Fisher Scientific, Carlsbad, CA, USA) following manufacturer's instructions. The concentrations of the extracted RNA were measured via a NanoDrop by absorption at 280 nm. The extracted mRNAs were loaded into an RNA Chip Kit and mRNA integrity was determined by automated electrophoresis using the Agilent 2100 Bioanalyzer (Santa Clara, CA, USA). The gel and corresponding electropherograms of the mRNA samples generated through the Agilent 2100 Expert Software (Agilent Technologies) were used to determine mRNA quality in the formulation following incubation in PBS or serum. The area under the curve for each sample (AUC_{FLUC-mRNA}) and timepoint was generated from the software and was normalized against the AUC_{FLUC-mRNA} at 0 h to give a normalized percentage area under the curve value (%AUC_{FLUC-mRNA}). The extracted mRNA samples (100 ng) were then incubated in wheat germ extract (Promega, Madison, WI, USA) containing 8U Ribolock inhibitor (Thermo Fisher Scientific, Mississauga, ON, Canada), 0.4 µL amino acid mix minus methionine (1 M) (Promega, Madison, WI, USA), and 0.4 µL amino acid mix minus cysteine (1 M) (Promega, Madison, WI, USA) at 25 °C for 1 h. Luciferase activity was measured using a luminometer (Turner Designs TD-20/20).

Statistical Analysis: All data were reported as the mean ± standard error of the mean (S.E.M.). Comparisons were made between distinct groups. Groups were analyzed by two-way analysis of variance (ANOVA) followed by a Tukey's post hoc correction, or two-tailed unpaired *t*-test. Statistical significance was set as * $p < 0.05$, ** $p < 0.01$, *** $p < 0.001$, and **** $p < 0.0001$, with a 95% confidence interval. Analysis and figures were generated using GraphPad Prism v. 7.0 and 9.0.

Supporting Information

Supporting Information is available from the Wiley Online Library or from the author.

Acknowledgements

M.H.Y.C. and J.L. contributed equally to this work. The authors thank Emma Kang and Lane Messier for their assistance with LNP formulations and cell culture, as well as Maryam Osooly for her assistance with the i.v. injections. The authors thank the UBC High Resolution Macromolecular Cryo-Electron Microscopy Facility (HRMEM) for support with cryo-TEM imaging. This work was funded by the Canadian Institutes for Health Research (FDN 148469). M.H.Y.C. was supported by a NanoMedicines Innovation Network postdoctoral fellowship award. J.L. was supported by a Frederick Banting and Charles Best Canada Graduate Scholarships Doctoral Award (no. 6557). D.W. was supported by the Swiss National Science Foundation (SNF Postdoc. Mobility Fellowship, grant no. 183923).

Conflict of Interest

P.R.C. has a financial interest in Acuitas Therapeutics and NanoVation Therapeutics as well as being Chair of NanoVation Therapeutics. A.A., X.Y., J.K., and D.W. are employees of NanoVation Therapeutics.

Data Availability Statement

The authors declares that the data from this study are available within the article and supplementary document upon request.

Keywords

bleb structures, lipid nanoparticles, mRNA delivery, phase separation

Received: April 13, 2023

Revised: May 10, 2023

Published online: June 25, 2023

- [1] M. H. Y. Cheng, C. A. Brimacombe, R. Verbeke, P. R. Cullis, *Mol. Pharmaceutics* **2022**, *19*, 1663.
- [2] A. Akinc, M. A. Maier, M. Manoharan, K. Fitzgerald, M. Jayaraman, S. Barros, S. Ansell, X. Du, M. J. Hope, T. D. Madden, B. L. Mui, S. C. Semple, Y. K. Tam, M. Ciufolini, D. Witzigmann, J. A. Kulkarni, R. van der Meel, P. R. Cullis, *Nat. Nanotechnol.* **2019**, *14*, 1084.
- [3] F. P. Polack, S. J. Thomas, N. Kitchin, J. Absalon, A. Gurtman, S. Lockhart, J. L. Perez, G. Perez Marc, E. D. Moreira, C. Zerbini, R. Bailey, K. A. Swanson, S. Roychoudhury, K. Koury, P. Li, W. V. Kalina, D. Cooper, R. W. Frenc, Jr., L. L. Hammitt, O. Tureci, H. Nell, A. Schaefer, S. Unal, D. B. Tresnan, S. Mather, P. R. Dormitzer, U. Sahin, K. U. Jansen, W. C. Gruber, C. C. T. Group, *N. Engl. J. Med.* **2020**, *383*, 2603.
- [4] E. Rohner, R. Yang, K. S. Foo, A. Goedel, K. R. Chien, *Nat. Biotechnol.* **2022**, *40*, 1586.
- [5] K. Musunuru, A. C. Chadwick, T. Mizoguchi, S. P. Garcia, J. E. DeNizio, C. W. Reiss, K. Wang, S. Iyer, C. Dutta, V. Clendaniel, M. Amaonye, A. Beach, K. Berth, S. Biswas, M. C. Braun, H. M. Chen, T. V. Colace, J. D. Ganey, S. A. Gangopadhyay, R. Garrity, L. N. Kasiewicz, J. Lavoie, J. A. Madsen, Y. Matsumoto, A. M. Mazzola, Y. S. Nasrullah, J. Nneji, H. Ren, A. Sanjeev, M. Shay, et al., *Nature* **2021**, *593*, 429.
- [6] J. D. Beck, D. Reidenbach, N. Salomon, U. Sahin, O. Tureci, M. Vormehr, L. M. Kranz, *Mol. Cancer* **2021**, *20*, 69.
- [7] J. G. Rurik, I. Tombacz, A. Yadegari, P. O. Mendez Fernandez, S. V. Shewale, L. Li, T. Kimura, O. Y. Soliman, T. E. Papp, Y. K. Tam, B. L. Mui, S. M. Albelda, E. Pure, C. H. June, H. Aghajanian, D. Weissman, H. Parhiz, J. A. Epstein, *Science* **2022**, *375*, 91.

- [8] J. A. Kulkarni, D. Witzigmann, S. B. Thomson, S. Chen, B. R. Leavitt, P. R. Cullis, R. van der Meel, *Nat. Nanotechnol.* **2021**, *16*, 630.
- [9] S. C. Semple, A. Akinc, J. Chen, A. P. Sandhu, B. L. Mui, C. K. Cho, D. W. Sah, D. Stebbing, E. J. Crosley, E. Yaworski, I. M. Hafez, J. R. Dorkin, J. Qin, K. Lam, K. G. Rajeev, K. F. Wong, L. B. Jeffs, L. Nechev, M. L. Eisenhardt, M. Jayaraman, M. Kazem, M. A. Maier, M. Srinivasulu, M. J. Weinstein, Q. Chen, R. Alvarez, S. A. Barros, S. De, S. K. Klimuk, T. Borland, et al., *Nat. Biotechnol.* **2010**, *28*, 172.
- [10] S. C. Semple, S. K. Klimuk, T. O. Harasym, N. Dos Santos, S. M. Ansell, K. F. Wong, N. Maurer, H. Stark, P. R. Cullis, M. J. Hope, P. Scherrer, *Biochim. Biophys. Acta* **2001**, *1510*, 152.
- [11] T. S. Zimmermann, A. C. Lee, A. Akinc, B. Bramlage, D. Bumcrot, M. N. Fedoruk, J. Harborth, J. A. Heyes, L. B. Jeffs, M. John, A. D. Judge, K. Lam, K. McClintock, L. V. Nechev, L. R. Palmer, T. Racie, I. Rohl, S. Seiffert, S. Shanmugam, V. Sood, J. Soutschek, I. Toudjarska, A. J. Wheat, E. Yaworski, W. Zedalis, V. Koteliensky, M. Manoharan, H. P. Vornlocher, I. MacLachlan, *Nature* **2006**, *441*, 111.
- [12] M. Jayaraman, S. M. Ansell, B. L. Mui, Y. K. Tam, J. Chen, X. Du, D. Butler, L. Eltepu, S. Matsuda, J. K. Narayanannair, K. G. Rajeev, I. M. Hafez, A. Akinc, M. A. Maier, M. A. Tracy, P. R. Cullis, T. D. Madden, M. Manoharan, M. J. Hope, *Angew. Chem., Int. Ed.* **2012**, *51*, 8529.
- [13] a) S. C. Semple, R. Leone, C. J. Barbosa, Y. K. Tam, P. J. C. Lin, *Pharmaceutics* **2022**, *14*, 398; b) Xinyao Du, S. M., Ansell, *US20160376224A1*, **2016**; c) K. E. Benenato, *US20170210697A1*, **2017**.
- [14] a) L. B. Jeffs, L. R. Palmer, E. G. Ambegia, C. Giesbrecht, S. Ewanick, I. MacLachlan, *Pharm. Res.* **2005**, *22*, 362; b) N. Maurer, K. F. Wong, H. Stark, L. Louie, D. McIntosh, T. Wong, P. Scherrer, S. C. Semple, P. R. Cullis, *Biophys. J.* **2001**, *80*, 2310; c) N. M. Belliveau, J. Huft, P. J. C. Lin, S. Chen, A. K. K. Leung, T. J. Leaver, A. W. Wild, J. B. Lee, R. J. Taylor, Y. K. Tam, C. L. Hansen, P. R. Cullis, *Mol. Ther.–Nucleic Acids* **2012**, *1*, e37.
- [15] J. A. Kulkarni, M. M. Darjuan, J. E. Mercer, S. Chen, R. van der Meel, J. L. Thewalt, Y. Y. C. Tam, P. R. Cullis, *ACS Nano* **2018**, *12*, 4787.
- [16] N. M. Belliveau, J. Huft, P. J. Lin, S. Chen, A. K. Leung, T. J. Leaver, A. W. Wild, J. B. Lee, R. J. Taylor, Y. K. Tam, C. L. Hansen, P. R. Cullis, *Mol. Ther.–Nucleic Acids* **2012**, *1*, e37.
- [17] J. A. Kulkarni, D. Witzigmann, J. Leung, R. van der Meel, J. Zaifman, M. M. Darjuan, H. M. Grisch-Chan, B. Thony, Y. Y. C. Tam, P. R. Cullis, *Nanoscale* **2019**, *11*, 9023.
- [18] M. L. Brader, S. J. Williams, J. M. Banks, W. H. Hui, Z. H. Zhou, L. Jin, *Biophys. J.* **2021**, *120*, 2766.
- [19] S. Arnott, R. Chandrasekaran, D. L. Birdsall, A. G. Leslie, R. L. Ratliff, *Nature* **1980**, *283*, 743.
- [20] J. W. Holland, C. Hui, P. R. Cullis, T. D. Madden, *Biochemistry* **1996**, *35*, 2618.
- [21] J. Gustafsson, H. Ljusberg-Wahren, M. Almgren, K. Larsson, *Langmuir* **1996**, *12*, 4611.
- [22] M. Packer, D. Gyawali, R. Yerabolu, J. Schariter, P. White, *Nat. Commun.* **2021**, *12*, 6777.
- [23] L. L. Yan, H. S. Zaher, *J. Biol. Chem.* **2019**, *294*, 15158.
- [24] a) U. F. Muller, Y. Tor, *Angew. Chem., Int. Ed.* **2014**, *53*, 5245; b) K. Adamala, J. W. Szostak, *Science* **2013**, *342*, 1098.
- [25] P. R. Cullis, B. de Kruijff, *Biochim. Biophys. Acta* **1979**, *559*, 399.